

Characterization of a liquid crystal microlens array using multiwalled carbon nanotube electrodes

Xiaozhi Wang,* Timothy D. Wilkinson, Mark Mann, Ken B. K. Teo, and William I. Milne

Electrical Engineering Division, University of Cambridge, 9 JJ Thompson Avenue, CB3 0FA, UK

*Corresponding author: xw224@mit.edu

Received 17 March 2010; revised 3 May 2010; accepted 9 May 2010;
posted 14 May 2010 (Doc. ID 125558); published 7 June 2010

Reconfigurable liquid crystal microlenses employing arrays of multiwalled carbon nanotubes (MWNTs) have been designed and fabricated. The cells consist of arrays of $2\ \mu\text{m}$ high MWNTs grown by plasma-enhanced chemical vapor deposition on silicon with a top electrode of indium tin oxide coated glass positioned $20\ \mu\text{m}$ above the silicon and the gap filled with the nematic liquid crystal BLO48. Simulations have found that, while its nematic liquid crystal aligns with MWNTs within a distance of $10\ \text{nm}$, this distance is greatly enhanced by the application of an external electric field. Polarized light experiments show that light is focused with focal lengths ranging from $\sim 7\ \mu\text{m}$ to $12\ \mu\text{m}$. © 2010 Optical Society of America

OCIS codes: 230.3720, 160.4236.

1. Background

A reconfigurable liquid crystal (LC) microlens array is useful in displays [1,2], integrated optics [3], and optical communications [4,5]. The traditional design of a microlens array consists of a zone-patterned structure, a hole or hybrid-patterned electrode, or a surface relief profile [6]. A new design and fabrication process for LC microlenses is proposed that incorporates an array of carbon nanotubes (CNTs) grown by plasma-enhanced chemical vapor deposition (PECVD) [7]. Vertically aligned multiwalled carbon nanotubes (MWNTs) grown on silicon or glass have been applied to field emission and field ionization [8,9] because of their strength and high aspect ratio, which causes significant electric field enhancement. Typical PECVD-grown MWNTs have diameters of $10\text{--}60\ \text{nm}$ and lengths of a few micrometers. Structurally, MWNTs consist of multiple rolled layers of graphene and always exhibit metallic-like electron transport. When an array of MWNTs is deposited between two parallel electrodes, such as in a capacitor, an applied potential will result in deformed and enhanced electric fields locally around the nanotubes, especially at their tips,

where field enhancement is maximized. This means that field emission and ionization occurs at the tips of the nanotubes for sufficiently high local fields. However, when applying a potential resulting in an electric field at the tips lower than the field emission threshold, no charge transfer occurs. At such lower potentials, a deformed static or alternating electrical field can be applied to align dipole or multipolar molecules to construct functional units and arrays. Theoretically, the microlens operates by aligning an anisotropic LC material in such a way that the refractive index is continuously varying from top to bottom and radially from the optical axis, thereby focusing light, as it is a graded index lenslet [10]. In this paper, a description and characterization of such a microlens is given both theoretically and experimentally.

2. Experiments

A CNT array was grown directly onto a silicon wafer by PECVD following the production of an array of Ni catalyst dots by a combined e -beam lithography and sputter coating process detailed elsewhere [11]. The diameter of a single MWNT is defined by the catalyst dot size. By increasing the size of the island, more than one MWNT can grow, and the number of MWNTs grown increases with the size of the island. It was

found that a single MWNT would grow from a catalyst site 100 nm to 200 nm in diameter by tuning the growth conditions. The substrate was heated by AC current at a pressure of 10^{-2} mbar to 650 °C at a ramping rate of 100 °C/min. A slow heating rate is preferred to protect catalyst dots from cracking. Ammonia was then introduced into the chamber through a showerhead to etch the surface of the Ni catalyst island. Acetylene was used as the carbon source and was added to the deposition chamber once the temperature reached 690 °C. A potential of 640 V DC was then applied between the gas showerhead and the heating stage to create a 40 W plasma. Growth for 10 to 15 min at 725 °C produces MWNTs with an average height of 4 μm , illustrated in Fig. 1. Because MWNT arrays are deposited onto a silicon wafer, they make the microlens a reflective optical device; however, a highly reflective back surface is preferred. Hence, a thin film of Al was deposited onto the top of the MWNT array so that the lens could be investigated. The top electrode is made of indium tin oxide (ITO) coated glass with an organic alignment layer spun onto the glass to which the LC molecules are aligned laterally. The silicon chip and top electrode were then pressed together with a gap of 20 μm defined by spacer balls. Before the device was sealed with UV glue, a positive, dielectric anisotropic nematic LC mixture (BLO48 from Merck) was fed in between the two electrodes.

3. Theoretical Calculations

It has been found that MWNTs have strong interactions with LC molecules [12–14]. To explore how the addition of MWNTs changes alignment in the LC upon the application of an electric field, *ab initio* calculations were performed using the Spanish Initiative for Electronic Simulations with Thousands of Atoms (SIESTA) [15]. To simplify the problem, a single walled carbon nanotube (SWNT) was simulated instead of a MWNT with the assumption that the outermost shell of a MWNT plays the most important role in interacting with the LC. The model consisted of two molecules, a perfect (5, 5) metallic SWNT and a simplified LC molecule. The molecules

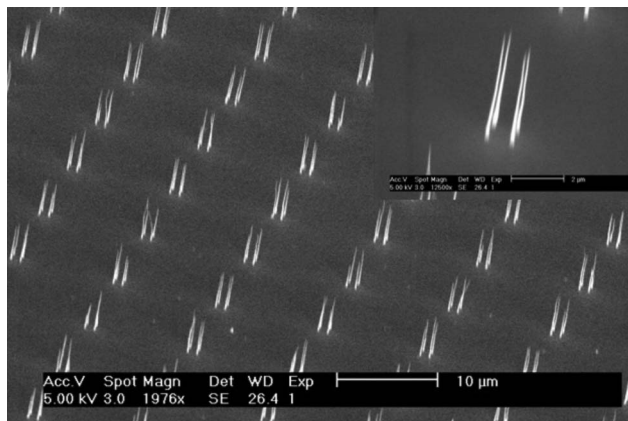


Fig. 1. Scanning electron microscopy (SEM) pictures for vertically aligned CNT arrays.

were kept at least 3 nm apart to prevent the formation of bonds. The simulation was constructed so that the positions of the atoms in the SWNT were fixed, given that MWNTs grown on the wafer are fixed. The LC molecules were allowed to move freely. For a constant intermolecular separation, three different geometries were simulated as shown in Fig. 2. For two geometries, the axis of the LC molecule was aligned perpendicular to the axis of the SWNT. In the third geometry, the axis of the LC molecule was aligned parallel to that of the SWNT. The total energy of the system for the three geometries was simulated for three different intermolecular separations, and a graph comparing the stability of the different configurations is plotted in Fig. 3. Subsequently, an external electrostatic field was then introduced into the models. The direction of the field applied was perpendicular to the axis of the SWNT. To obtain a geometry equivalent to the lens described above, the magnitude of the field applied was $5 \times 10^4 \text{ V m}^{-1}$, which was equal to the field generated between two parallel plates with a separation of 20 μm and a potential difference of 1 V. It was found that after introducing a particular external field, the LC molecule rotated un-

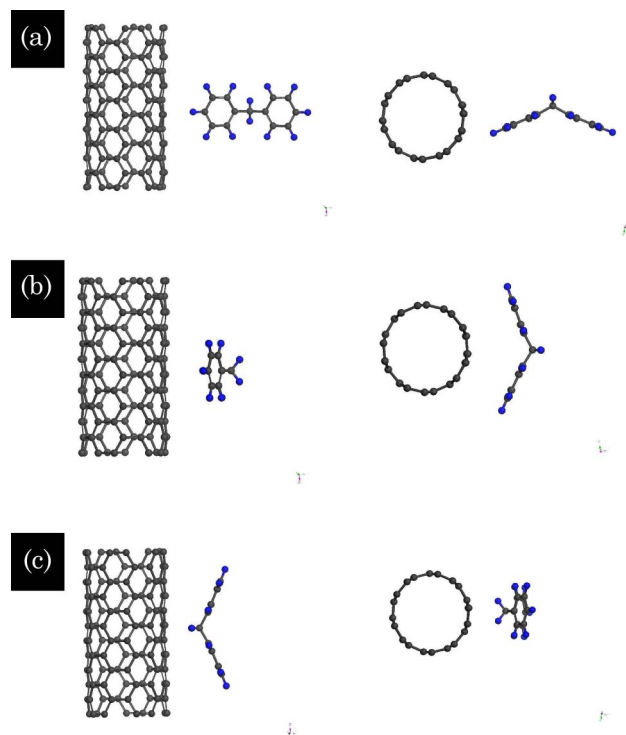


Fig. 2. (Color online) Model consists of a SWNT and a simplified LC molecule. The LC molecule has two benzene rings bridged by a carbon atom. The axis of this molecule is assumed to be in the same direction as the line connecting the center of two benzene rings. (a), (b), and (c) show both the cross view and top view. (a) The axis of LC molecule is perpendicular to and in the same plane as the axis of SWNT. (b) The axis of LC molecule is perpendicular to but in a different plane from the axis of SWNT. (c) The axis of LC molecule is parallel to the axis of SWNT. The distance between LC molecule and SWNT is defined to be between the nearest two carbon atoms in them respectively. Calculations are conducted for (a), (b), and (c) for distances between two molecules from 2 nm to 8 nm.

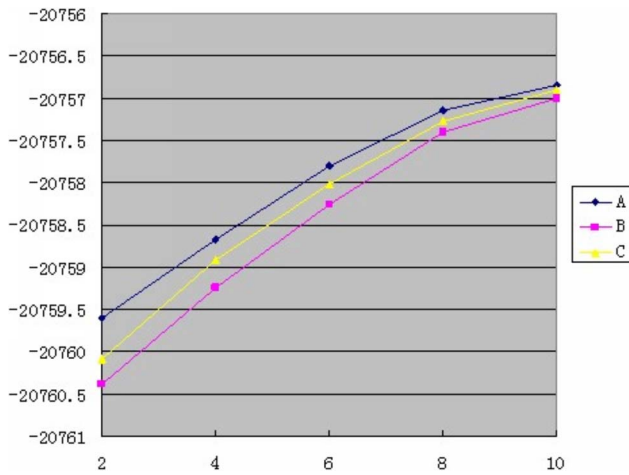


Fig. 3. (Color online) Total system energy curves A, B, C correspond to Figs. 2(a)–2(c), respectively. It can be noticed that the model shown as Fig. 2(b) has the lowest total energy, which means LC can be aligned by SWNT in such form without an electrical field. When the distance between two increases, the energy difference between any two of those three different systems becomes smaller. Thus when distance is further than 10 nm, it can be assumed that SWNT cannot align LC itself.

til the most stable energetic configuration was found. This occurs when the LC molecule orientates itself parallel to the field direction. This calculation indicates that a LC will align with an electrical field in the ON state.

Finite element calculations (FEM) were used to determine the profile of the electrical field generated by a MWNT and hence the profile of a LC microlens. Because the MWNTs were small, the lens effect was too small to be seen clearly due to lateral confinement at the background field. Therefore, the lens effect needs to be boosted to prevent the effect from being too localized. It was found that when two MWNTs were separated by less than half their height, their localized fields merged, which is shown in Fig. 4(a). This means that the effective field was nearly doubled parallel to the substrate surface. To extend this effect into three dimensions, four MWNTs were combined to form one lens profile, and the top view of the electrical field at varying heights above the tips of the MWNTs is presented in Figs. 4(b) to 4(f). It can be seen that the electrical field lines are still centered on the central MWNTs. Therefore the lens profile and the difference in the refractive index were preserved.

4. Results

As demonstrated in [10], the LC lens aperture is effectively expanded by combining four MWNTs in a cluster. A polarizing microscope was used to focus on a plane between the two electrodes within the cell. Figure 5 shows how increasing the voltage affects the focal plane. The black dots indicate the locations of vertical MWNT units, and each unit is spaced by $10 \mu\text{m}$. The clearest image of the MWNTs can be

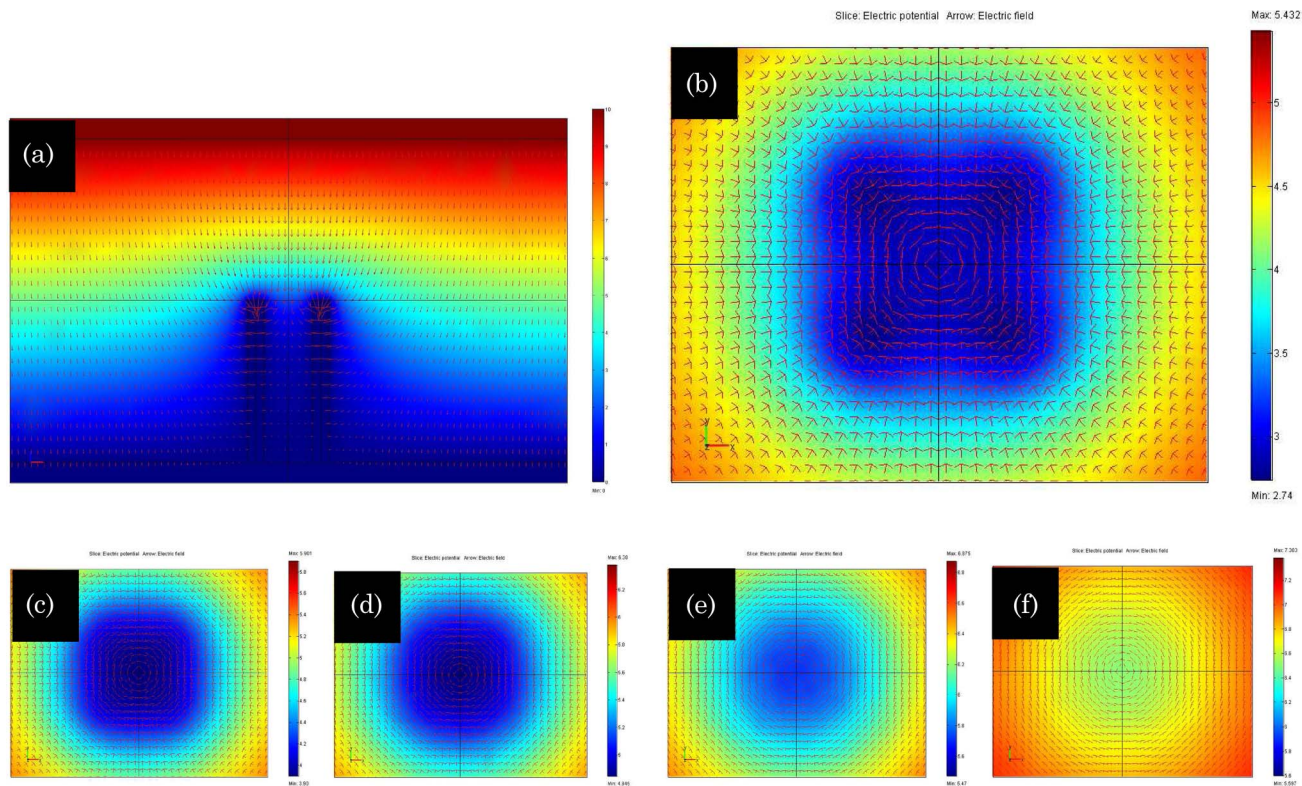


Fig. 4. (Color online) FEM consists of four vertical conductive rods with length of $10 \mu\text{m}$ that stand together spaced by less than half of their length as shown in (a). There are two parallel planar electrodes apart from each other, twice of the length of rods, which is $20 \mu\text{m}$. 10 V is applied between them to generate DC field. (b) to (f), Top views of electrical field in different heights, from just above rods apex to near top electrode with the planar dimension of $30 \mu\text{m} \times 20 \mu\text{m}$. The heights from (b) to (f) are $11 \mu\text{m}$, $13 \mu\text{m}$, $15 \mu\text{m}$, $17 \mu\text{m}$, and $19 \mu\text{m}$, respectively.

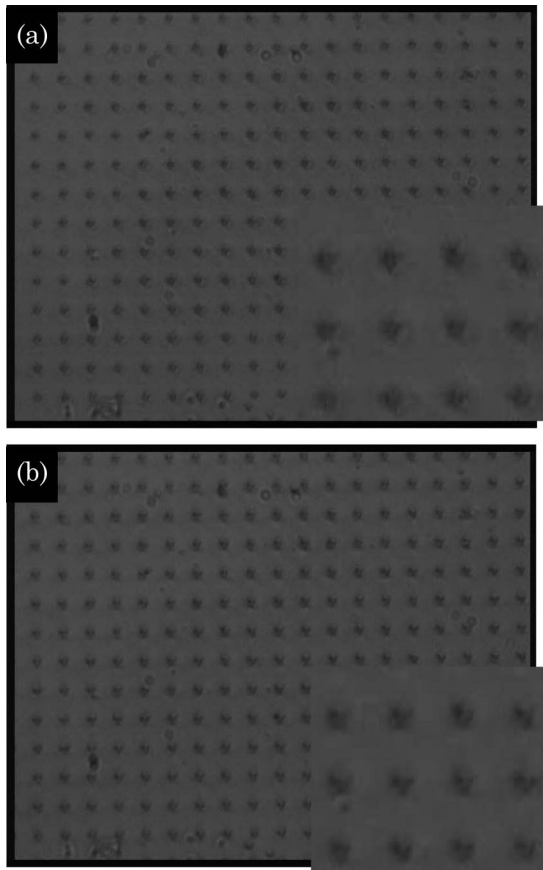


Fig. 5. (a) MWNT focused by adjusting the voltage before voltage reaches the focal point for MWNT imaging. (b) Single MWNT is focused.

found under a voltage. It was found that when the focal plane was altered, a different voltage was needed to focus the MWNTs again. It is found that the MWNTs can be focused and use voltage from 1 V to 6 V. The alignment of the LC can also be confirmed by the focusing of the MWNTs. Figure 6(a) shows a picture taken with the microscope without using a polarizer or an applied electrical field. The areas around the MWNTs are dark in all directions because of an LC defect. The LC layer is aligned not only by the alignment layer on the glass but also by the MWNTs with the effect simulated in Figs. 2 and 3. Because of this, light is absorbed in more polarization directions; hence it appears darker around the MWNTs. After applying a voltage, an effective microlens unit can be divided into four different areas as can be seen in Fig. 6(b). Using polarizers in the microscope, one can see that areas above and below the MWNT locations are brighter, while areas to the left and right of the MWNTs are black. This is because the LC molecules all point toward the central MWNTs upon application of a field as simulated in Fig. 4. Consequently the reflected light, polarized by these aligned LC molecules, only passes through the polarizers at two points 180° apart. When shifting the microscope focus with a fixed voltage, a bright array of dots appeared in a certain plane between the

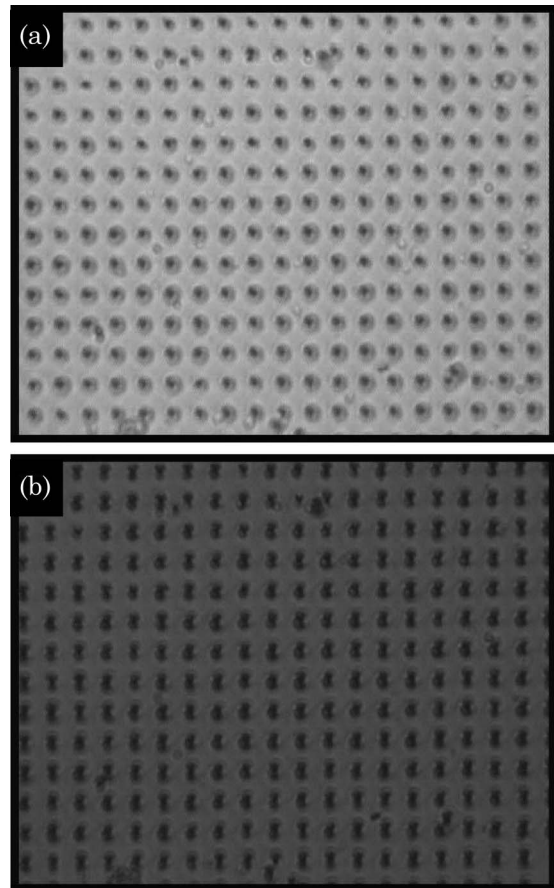


Fig. 6. (a) Picture taken in microscope without polarization and applied voltage. (b) Picture taken with polarized light and applied voltage.

two electrodes, as shown in Fig. 7(a). Once the array of bright dots was found, the voltage between the two electrodes was adjusted over a small range of a few volts. The bright dots became blurred [Fig. 7(b)], which were then refocused by adjusting the microscope's focal length. This was because when varying the voltage, the electrostatic field profile of the microlens changed, and hence the focal length was modified. Consequently, a new focal plane was required to see reflected light again. Both experiments demonstrated that one can focus reflected light by varying either the field or the microscope's focal length.

Fresnel's approximation can be used to calculate the approximate focal length of this microlens:

$$f = \frac{(D/2)^2}{2\delta n t}, \quad (1)$$

where D is the lens aperture, δn is the difference in the refractive index between the center of the lens (where the MWNT is grown) and the edge of the microlens, and t is the electrode gap, which is 20 μm in our case. The edge of the microlens can be tuned by the electrical field; for instance, the LC molecules will be aligned further from the MWNTs at higher voltages. Therefore, from Eq. (1), there are two

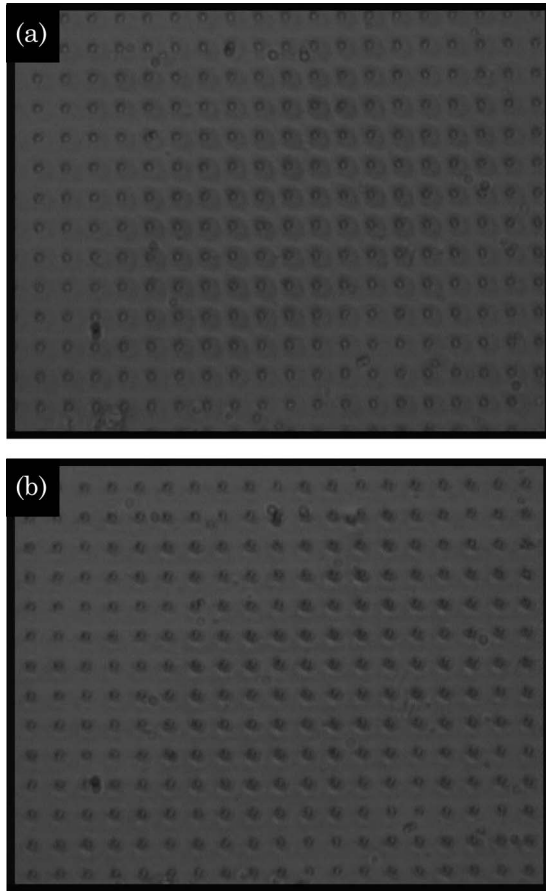


Fig. 7. (a) Bright dots in the middle of black dots shows the focalization of reflected light. (b) By adjusting voltage in small range, bright dots become out of focus if the microscope lens keeps the same position.

factors that can be tuned to change the lens' focus, D and δn . The shortest focal length occurs when $D/\delta n$ is a minimum, though the diameter of the lens cannot be too large because the LC needs to be aligned parallel to the planar electrodes at the center but as perpendicular as possible to the electrodes at the edge of the microlens. Ideally, one should be able to tune the focal plane from infinity to a certain distance by turning on the field, moving the focal plane, and then enlarging the border by increasing the field. When δn is ~ 0.1 and D is $\sim \mu\text{m}$, adjusted by the voltage, the focal length is in micrometers. The focal length was measured with different applied voltages. As shown in Table 1, the focal length is around $7 \mu\text{m}$ at 1 V and varies when voltage increases due to the aperture and the refractive index difference variation.

5. Summary

To summarize, after designing a new CNT based LC microlens with a diameter of less than $10 \mu\text{m}$, we have fabricated and demonstrated the focusing of light. Alignment of the LC was predicted by simulation and confirmed with a polarized microscope.

Table 1. Focal Length of Microlens Adjusted by Voltage

| Applied Voltage (V) | 1 | 2 | 3 | 4 | 5 | 6 |
|--------------------------------|-----|-----|------|------|-----|----|
| Focal Length (μm) | 7.3 | 9.1 | 11.1 | 10.3 | 9.4 | 12 |

Without an electric field, the focal length of the microlens is infinite due to the parallel plane electrodes and homogeneous LC alignment. An electric field can be applied to gradually tune the focal length. By patterning the CNT growth, a microlens array can be fabricated, and lens profiles can be varied.

References

1. T. Nose and S. Sato, "LCD devices obtained using scattering properties of microlens effects," *Proc. Soc. Inf. Disp.* **32**, 177–181 (1991).
2. S. Sato, "Applications of liquid crystals to variable-focusing lenses," *Opt. Rev.* **6**, 471–485 (1999).
3. Y. Zhang, Y. Li, E. G. Kanterakis, A. Kats, X. J. Lu, R. Tolimieri, and N. P. Cavouris, "Optical realization of wavelet transform for a one-dimensional signal," *Opt. Lett.* **17**, 210–212 (1992).
4. T. Nose and S. Sato, "Optical properties of liquid-crystal microlens," *Proc. SPIE* **1230**, 17 (1990).
5. T. Nose and S. Sato, "Application of liquid crystal microlens in optical fiber switch," *Trans. IEICE* **75-C1**, 155–163 (1992) (in Japanese).
6. T. Nose and S. Sato, "A liquid crystal microlens obtained with a non-uniform electric field," *Liq. Cryst.* **5**, 1425–1433 (1989).
7. K. B. K. Teo, M. Chhowalla, G. A. J. Amaratunga, W. I. Milne, D. G. Hasko, G. Pirio, P. Legagneux, F. Wyczisk, and D. Pribat, "Uniform patterned growth of carbon nanotubes without surface carbon," *Appl. Phys. Lett.* **79**, 1534–1536 (2001).
8. W. I. Milne, K. B. K. Teo, M. Chhowalla, G. A. J. Amaratunga, S. B. Lee, D. G. Hasko, H. Ahmed, O. Groening, P. Legagneux, L. Gangloff, J. P. Schnell, G. Pirio, D. Pribat, M. Castignolles, A. Loiseau, V. Semet, and V. T. Binh, "Electrical and field emission investigation of individual carbon nanotubes from plasma enhanced chemical vapour deposition," *Diamond Relat. Mater.* **12**, 422–428 (2003).
9. A. Modi, N. Koratkar, E. Lass, B. Wei, and P. M. Ajayan, "Miniaturized gas ionization sensors using carbon nanotubes," *Nature* **424**, 171 (2003).
10. T. Wilkinson, X. Wang, K. B. K. Teo, and W. I. Milne, "Sparse multiwall carbon nanotube electrode arrays for liquid-crystal photonic devices," *Adv. Mater.* **20**, 363–366 (2008).
11. K. B. K. Teo, E. Minoux, L. Hudanski, F. Peauger, J.-P. Schnell, L. Gangloff, P. Legagneux, D. Dieumgard, G. A. J. Amaratunga, and W. I. Milne, "Microwave devices: carbon nanotubes as cold cathodes," *Nature* **437**, 968 (2005).
12. I. Dierking, G. Scalia, and P. Morales, "Liquid crystal-carbon nanotube dispersions," *J. Appl. Phys.* **97**, 044309 (2005).
13. C. Y. Huang, C. Y. Hu, and H. C. Pan, "Electrooptical responses of carbon nanotube-doped liquid crystal devices," *Jpn. J. Appl. Phys.* **44**, 8077–8081 (2005).
14. I. S. Baik, S. Y. Jeon, and S. H. Lee, "Electrical-field effect on carbon nanotubes in a twisted nematic liquid crystal cell," *Appl. Phys. Lett.* **87**, 263110 (2005).
15. J. M. Soler, E. Artacho, J. D. Gale, A. García, J. Junquera, P. Ordejón, and D. Sánchez-Portal, "The SIESTA method for *ab initio* order- N materials simulation," *J. Phys. Condens. Matter* **14**, 2745–2779 (2002).